The Global ECT-MRI Research Collaboration (GEMRIC)

Oltedal, Leif; Bartsch, Hauke; Sørhaug, Ole Johan Evjenth; Kessler, Ute; Abbott, Christopher; Dols, Annemieke; Stek, Max L; Ersland, Lars; Emsell, Louise; van Eijndhoven, Philip; Argyelan, Miklos; Tendolkar, Indira; Nordanskog, Pia; Hamilton, Paul; Jorgensen, Martin Balslev; Sommer, Iris E; Heringa, Sophie M; Draganski, Bogdan; Redlich, Ronny; Dannlowski, Udo; Kugel, Harald; Bouckaert, Filip; Sienaert, Pascal; Anand, Amit; Espinoza, Randall; Narr, Katherine L; Holland, Dominic; Dale, Anders M; Oedegaard, Ketil J

Published in:
NeuroImage: Clinical

DOI:
10.1016/j.nicl.2017.02.009

Publication date:
2017

Document version
Publisher's PDF, also known as Version of record

NeuroImage: Clinical 14 (2017) 422–432

Contents lists available at ScienceDirect

NeuroImage: Clinical

journal homepage: www.elsevier.com/locate/ynicl

The Global ECT-MRI Research Collaboration (GEMRIC): Establishing a multi-site investigation of the neural mechanisms underlying response to electroconvulsive therapy

Leif Oltedal[a,b,c,d,*,1], Hauke Bartsch[b,c], Ole Johan Evjenth Sørhaug[a], Ute Kessler[a,e], Christopher Abbott[f], Annemieke Dols[g], Max L Stek[g], Lars Ersland[h], Louise Emsell[i], Philip van Eijndhoven[j], Miklos Argyelan[k], Indira Tendolkar[j], Pia Nordanskog[l], Paul Hamilton[l], Martin Balslev Jorgensen[m], Iris E Sommer[n], Sophie M Heringa[n], Bogdan Draganski[o,p], Ronny Redlich[q], Udo Dannlowski[q,r], Harald Kugel[s], Filip Bouckaert[t], Pascal Sienaert[t], Amit Anand[u], Randall Espinoza[v], Katherine L Narr[v,w], Dominic Holland[b,x], Anders M Dale[b,c,x], Ketil J Oedegaard[a,e,y]

[a] Department of Clinical Medicine, University of Bergen, Bergen, Norway
[b] Center for Multimodal Imaging and Genetics, University of California, San Diego, La Jolla, CA, USA
[c] Department of Radiology, University of California, San Diego, La Jolla, CA, USA
[d] Department of Radiology, Haukeland University Hospital, Bergen, Norway
[e] Division of Psychiatry, Haukeland University Hospital, Bergen, Norway
[f] Department of Psychiatry, University of New Mexico School of Medicine, Albuquerque, USA
[g] VUmc Amsterdam/GGZinGeest, Amsterdam, Netherlands
[h] Department of Clinical Engineering, Haukeland University Hospital, Bergen, Norway
[i] KU Leuven, University Psychiatric Center KU Leuven, Leuven, Belgium
[j] Donders Institute for Brain, Cognition and Behavior, Department of Psychiatry, Nijmegen, Netherlands
[k] Center for Psychiatric Neuroscience, Feinstein Institute for Medical Research, New York, USA
[l] Center for Social and Affective Neuroscience, Department of Clinical and Experimental Medicine, Faculty of Health Sciences, Linköping University, Linköping, Sweden.
[m] Psychiatric Center Copenhagen, Copenhagen, Denmark
[n] Brain Center Rudolf Magnus, University Medical Center, Utrecht, Utrecht, Netherlands
[o] LREN, Department of Clinical Neurosciences – CHUV, University Lausanne, Switzerland
[p] Max-Planck-Institute for Human Brain and Cognitive Neurosciences, Leipzig, Germany
[q] Department of Psychiatry, University of Münster, Germany
[r] Department of Psychiatry, University of Marburg, Germany
[s] Department of Clinical Radiology, University of Münster, Germany
[t] KU Leuven, University Psychiatric Center KU Leuven, Academic center for ECT and Neurostimulation (AcCENT), Kortenberg, Belgium.
[u] Cleveland Clinic, Center for Behavioral Health, Cleveland, USA
[v] Department of Psychiatry and Biobehavioral Sciences, University of California, Los Angeles (UCLA), CA, USA
[w] Department of Neurology, University of California, Los Angeles (UCLA), CA, USA
[x] Department of Neurosciences, University of California, San Diego, La Jolla, CA, USA
[y] K.G. Jebsen Centre for Research on Neuropsychiatric Disorders, Bergen, Norway

ARTICLE INFO

Article history:
Received 15 December 2016
Received in revised form 9 February 2017
Accepted 10 February 2017
Available online 14 February 2017

Keywords:
Electroconvulsive therapy
MRI
Longitudinal
Mega analysis
Multi-site

ABSTRACT

Major depression, currently the world's primary cause of disability, leads to profound personal suffering and increased risk of suicide. Unfortunately, the success of antidepressant treatment varies amongst individuals and can take weeks to months in those who respond. Electroconvulsive therapy (ECT), generally prescribed for the most severely depressed and when standard treatments fail, produces a more rapid response and remains the most effective intervention for severe depression. Exploring the neurobiological effects of ECT is thus an ideal approach to better understand the mechanisms of successful therapeutic response. Though several recent neuroimaging studies show structural and functional changes associated with ECT, not all brain changes associate with clinical outcome. Larger studies that can address individual differences in clinical and treatment parameters may better target biological factors relating to or predictive of ECT-related therapeutic response. We have thus formed the Global ECT-MRI Research Collaboration (GEMRIC) that aims to combine longitudinal neuroimaging as well as clinical, behavioral and other physiological data across multiple independent sites. Here, we summarize the

* Corresponding author at: Center for Multimodal Imaging and Genetics, University of California, San Diego, 9452 Medical Center Drive, La Jolla, CA 92037, USA.
E-mail address: leif.oltedal@uib.no (L. Oltedal).
[1] Permanent address: Department of Clinical Medicine, University of Bergen, Bergen, Norway.

http://dx.doi.org/10.1016/j.nicl.2017.02.009

ECT sample characteristics from currently participating sites, and the common data-repository and standardized image analysis pipeline developed for this initiative. This includes data harmonization across sites and MRI platforms, and a method for obtaining unbiased estimates of structural change based on longitudinal measurements with serial MRI scans. The optimized analysis pipeline, together with the large and heterogeneous combined GEMRIC dataset, will provide new opportunities to elucidate the mechanisms of ECT response and the factors mediating and predictive of clinical outcomes, which may ultimately lead to more effective personalized treatment approaches.

1. Introduction

Depressive disorders are now the single leading cause of disability worldwide (Whiteford et al., 2013). Though several treatments for depression are available, these are not successful in all individuals (Rush et al., 2006). Electroconvulsive therapy (ECT) is the most effective acute treatment of major depressive episodes (Carney et al., 2003), but remains stigmatized (Aoki et al., 2016). Clinical indications and other criteria for ECT are well articulated by various international scientific and professional bodies (APA, 2001; Kennedy et al., 2009; NICE, 2009). Due to the potential for cognitive side-effects and limited availability, ECT is typically only considered indicated for the most severely depressed or in otherwise treatment-resistant patients. Research aimed at targeting changes in brain function and morphology with ECT, which elicits a more rapid onset of action than standard therapies, may help resolve the complex mechanisms underlying successful clinical response as well as those accounting for side-effects. Specific knowledge on how ECT alleviates depression, and its impact on brain anatomy and function, should help clinicians and patients make informed choices regarding the use of ECT to treat the illness, and reduce the stigma associated with the treatment. More importantly, new knowledge may lead to the development of better and more targeted personalized treatments.

Longitudinal neuroimaging studies, i.e. with imaging of patients before- and after ECT, have already shown that ECT has effect on specific brain regions and circuits. The first of such MRI-studies appeared in the late 1980s (Coffey et al., 1988; Figiel et al., 1989; Mander et al., 1987). Hindered by poor resolution (typical slice thickness 5–12 mm, inter slice interval 1–2.5 mm), low field strength (0.08, 1 or 1.5 T), and limited tools for quantification or automated image processing, these studies were primarily focused on disproving the hypothesis that ECT causes brain damage. Structural changes or gross evidence of harmful effects was not found (Coffey et al., 1988; Figiel et al., 1989; Pande et al., 1990; Puri et al., 1998). However, ECT-induced changes in tissue parameters, such as an increase in T1- and T2 relaxation times (Mander et al., 1987; Scott et al., 1990) were reported. As these findings may be related to increased brain water content, it was speculated that changes in T1 relaxation time could be caused by breakdown of the blood-brain barrier or related to anesthesia (Mander et al., 1987), but partial volume effects with CSF, causing an apparent change in T1-or T2 relaxation times could not be ruled out (Scott et al., 1990). Subsequent investigations showed conflicting results, confirming (Diehl et al., 1994) and not confirming (Girish et al., 2001; Kunigiri et al., 2007) the change in T2 relaxation times. One study also reported an increase in the number of T2 hyperintensities, a finding related to atherosclerotic small vessel disease, for a few elderly patients 6 months after treatment (Coffey et al., 1991).

Interestingly, after the first high-resolution (1 mm^3) MRI study identified ECT-induced structural changes by detecting increased volume of the hippocampus (Nordanskog et al., 2010), several subsequent studies have confirmed that ECT induces structural changes in the hippocampus as well as other brain areas (Abbott et al., 2014; Bouckaert et al., 2016a; Dukart et al., 2014; Jorgensen et al., 2016; Joshi et al., 2016; Ota et al., 2015; Redlich et al., 2016; Sartorius et al., 2016; Tendolkar et al., 2013). For example, both Tendolkar et al. and Joshi et al. found bilateral volume increase in hippocampus and amygdala; Abbott et al., Dukart et al. and Ota et al. demonstrated significant volume increase of the right hippocampus only; Bouckaert et al. found volume increases in the caudate nucleus and in the medial and superior temporal lobe ipsilateral to the stimulation side; Dukart et al. also reported areas of volume decrease. Sartorius et al. found increase in whole-brain gray matter volume after ECT, with the most prominent change in the right temporal lobe. One study reported no ECT-induced changes (Nickl-Jockschat et al., 2016). In summary, with improvements in imaging techniques, ECT-induced structural brain changes have been documented, and the focus of investigations has moved towards exploring signs of ECT-stimulated neuroplasticity. Evidence for this hypothesis comes from animal studies that show neuroplastic effects with electroshock (see e.g. (Bouckaert et al., 2014; Segi-Nishida, 2011) for reviews). However, animal models are not necessarily transferable to humans, and it is currently unclear how ECT-induced brain changes relate to treatment outcome (Bouckaert et al., 2016b; Jorgensen et al., 2016; Redlich et al., 2016). Further, results in humans are only partially consistent and may depend on ECT stimulus and patient characteristics particular to each study. Although single-site investigations tend to have carefully selected samples, they struggle with limited power, and may have limited data analysis methods.

Major depression is a clinically heterogeneous disorder and a host of individualized clinical, biological and treatment-related factors (e.g., age, severity/length of illness, particular neuropsychological profiles, treatment parameters etc.) may account for varied therapeutic response. Only large sample sizes can address how variations in particular brain circuits relate to such factors and/or impact clinical outcome. Likewise, only large samples may address the relationships between changes in neural structure and function to dissociate epiphenomena and antidepressant response mechanisms. Notably, the identification of objective biological markers extracted from neuroimaging data that could predict future clinical response could transform clinical practice. However, to train and test predictive models that incorporate and are sensitive to individual differences in demographic, clinical and treatment factors also requires large datasets.

More than 50% of scientists have experienced failure to reproduce results, and low statistical power is reported as one of the main reasons (Baker, 2016). Differences in sample characteristics and methodological approaches across single site studies combined with the examination of small samples can impact the reproducibility of findings. In meta-analysis, summary measures (not individual patient data) from multiple sites are combined for statistical analysis. Several meta-analyses of cross-sectional MRI data in major depressive disorder (MDD) exist, where reductions in hippocampal volume in MDD compared to controls appears the most consistent finding (Arnone et al., 2016; Boccia et al., 2015; Bora et al., 2012; Campbell et al., 2004; Cole et al., 2011; Du et al., 2014; Hamilton et al., 2008; Kempton et al., 2011; Koolschijn et al., 2009; McKinnon et al., 2009; Peng et al., 2016; Sexton et al., 2013; Steele et al., 2007; Videbech and Ravnkilde, 2004; Zhao et al., 2014). However, with meta-analyses, the methodology across studies is under less control, individual-subject level data is lacking and it is more difficult to perform additional analyses to explore novel hypotheses. In mega-analysis, on the other hand, data from each individual patient is combined in a single database for common analysis. This

requires relative homogeneity of the data quality across studies and is usually a more time consuming approach. However, the added advantage is that all subject level data are present in the same database which allows investigators to address a much broader set of hypotheses, and in studies where multivariate data is handled (eg. genetics, neuroimaging, clinical, etc.) refining a model by incorporating a new covariate (e.g. age or total intracranial volume) can be easily achieved. In addition, studies on individual patient diagnosis, prognosis or prediction, e.g. machine or deep learning approaches, are possible. In Table 1 we summarize relevant differences between single site studies, meta- and mega analysis for the study of ECT-related brain effects.

To allow for mega-analysis of the neural mechanisms and predictors of ECT-related clinical response, this paper describes the formation of an international collaboration, termed the Global ECT-MRI Research Collaboration (GEMRIC), with the goal of creating a large database of multi-site imaging data and clinical/behavioral/physiological and metadata for analysis of the neural mechanisms and predictors of ECT-related clinical response. Although the unique and complementary biological information afforded by different imaging modalities (structural, functional, diffusion and perfusion MRI, and magnetic resonance spectroscopy) is expected to provide a more comprehensive understanding of the mechanisms of ECT, the initial goal of the GEMRIC is to develop analysis and datamining approaches for structural MRI data followed with other imaging modalities in the future.

Large international multi-center research studies such as the Alzheimers's Disease Neuroimaging Initiative (ADNI) (Jack et al., 2008), and the wide availability of common analysis tools, such as FreeSurfer, has paved the way for some general standardization of acquisition protocols and analysis methods. That is, contemporary structural MRI data is typically acquired with high resolution 3D sequences, which allows for standardized processing pipelines, even without additional a priori defined and standardized imaging sequence parameters. This allows large numbers of subjects to be analyzed with consistent analysis pipelines, which is an objective of GEMRIC. Consequently, rigorous testing of the relationship between the "experimental" manipulation (e.g. ECT parameters), and brain and health effects may be examined.

Below we present our process of identifying potential contributors for this international collaboration and the roadmap for establishing goals for future investigations and new collaborations. Finally, we characterize our current GEMRIC dataset, describe the tools for common data analysis and evaluate our initial processing pipeline for handling data collected across MRI systems.

2. Methods

The methods for setting up the GEMRIC included 1) identifying contributing investigative groups, 2) establishing collaborative and data sharing agreements, 3) developing a common data portal, 4) developing and testing a structural image preprocessing pipeline, and 5) standardization of multi-site clinical data.

Table 1
Research designs for studying ECT-related brain effects.

	Single site	Multi-site (Meta)	Multi-site (Mega)
Sample size	10–100[a]	100–1000	100–1000
Patient sample	Homogeneous	Heterogeneous	Heterogeneous
ECT stimulus parameters	Homogeneous	Heterogeneous	Heterogeneous
Variance in software/analysis tools	NO	YES/NO[b]	NO
Individual-subject level prediction	YES	NO	YES
Detecting rare events	NO	NO	YES

[a] Numbers typical for longitudinal studies of ECT.
[b] Some meta-analysis, like ENIGMA, exclude this variance by using consistent analysis pipelines across sub-studies.

To identify contributing groups, a systematic search in Medline, Embase and PsycInfo was undertaken (September 2014) to target studies that included imaging measurements before and after ECT (see Inline Supplementary material for exact search terms); 2153 papers were identified of which 94 included imaging measurements both before *and* after ECT. Of 34 studies that used MRI, four different modalities were used; structural (T1, T2; 15), functional (Bold fMRI; 5), spectroscopy (H MRS; 11) and diffusion (DWI/DTI; 3). In total 13 studies included volumetric T1 acquisitions with a minimum resolution of 1.3 mm in any direction (see Inline Supplementary Fig. S1), and the 11 corresponding authors of these papers were contacted by email in November 2014.

Inline Supplementary Fig. S1 can be found online at http://dx.doi.org/10.1016/j.nicl.2017.02.009.

To facilitate data sharing, guidelines and agreements for collaboration were established under the guidance of site-specific institutional review boards (IRBs). Next, a common data portal was created to allow individual sites to import raw DICOM data to a common server. An advantage of processing raw data on a common portal (versus transferring processed data) is that differences in software installations are eliminated, and quality control are the same across independent datasets (Bartsch et al., 2014). A processing pipeline for automated longitudinal analysis of individual patient data was then set up on this common analysis platform. The pipeline includes corrections for scanner-specific effects using a gradient unwarp tool that corrects 3D T1 data for effects of scanner-dependent gradient field non-linearities (Jovicich et al., 2006). Then the individual brain MRI is processed using automated FreeSurfer preprocessing steps (version 5.3; surfer.nmr.mgh.harvard.edu/), which includes segmentation of subcortical white matter, deep gray matter structures and automated parcellation of the cerebral cortex (Dale and Sereno, 1993; Desikan et al., 2006; Fischl et al., 2002; Fischl et al., 2004). Next, unbiased, within-subject assessment of longitudinal changes of regional brain volumes is performed using Quarc (Holland et al., 2009; Holland and Dale, 2011; Holland et al., 2012). In summary, this pipeline builds on lessons from prior studies (notably ADNI) by correcting for scanner-specific distortions and using methods that maximize power for longitudinal change estimation while avoiding bias (Fox et al., 2011; Holland et al., 2012; Thompson et al., 2011).

The current GEMRIC sample is described in the results section. However, a selected sample from one site (Bergen; $n = 19$ patients and $n = 9$ controls), was used to test feasibility, and to evaluate the image analysis processing pipeline. The work was carried out in accordance with The Code of Ethics of the World Medical Association (Declaration of Helsinki) for medical research involving human subjects. Here, 19 patients in a major depressive episode receiving right unilateral ECT (age: 48.0 ± 16.6, 63% female) underwent the exact same research protocol (Oltedal et al., 2015a) but two different scanners were used: Six patients were scanned on a 3T GE Signa HDxt equipped with an 8-channel head coil. The protocol included a T1-weighted inversion recovery spoiled gradient echo sequence, IR SPGR (TE/TR = 2.8/6.5 ms; TI = 450 ms; flip angle = 8°; FOV 256 mm; voxel size = $1.0 \times 1.0 \times 1.0$ mm^3), and the remaining 13 patients were scanned on a GE Discovery MR750 3T equipped with a 32-channel head coil. The protocol included a fast spoiled gradient echo, FSPGR (TI = 600 ms; flip angel = 8; TE/TR = 2.9/6.7 ms; FOV256 mm; voxel size = $1.0 \times 1.0 \times 1.0$ mm^3). After unwarping, both corrected (i.e. unwarped) and uncorrected 3D volumes were analyzed manually and automatically with FreeSurfer ($n = 6$ subjects at each scanner). Automatic segmentation of subcortical volumes was then statistically compared within groups, assessed by Student's two-tailed paired *t*-tests. For the unbiased regional change analysis, Quarc was ran on data both before- and after the gradient unwarp step from all 19 subjects with scans from before- and after ECT, and 9 healthy controls with scans at similar time intervals. Student's two sample two-tailed *t*-tests were used when comparing patients and controls. Cohen's *d* was calculated as dv/SD where dv represents the mean change estimate and SD the standard deviation of a

given region of interest (ROI). Results were considered statistically significant at the $P < 0.05$ level. Data are presented as mean ± Standard Deviation (SD). Sample size was estimated by using the software package G * Power (version 3.1.9.2) (Faul et al., 2007), and for these analyses Cohen's *d* was calculated from the mean of the estimated regional anatomical change from the left and right hemisphere.

Finally, since different sites included different mood rating scales from completed or current investigations, methods were implemented to allow for the standardization of multi-site clinical data for GEMRIC.

3. Results

3.1. Forming the collaboration

After identifying potential contributors to the GEMRIC through the literature search described above, 7 of the 11 contacted authors joined the collaborative group. Through additional contacts within this set of investigators, an additional 8 sites agreed to participate so that currently 15 independent groups - including the imaging core at UCSD - make up the GEMRIC (Fig. 1). Three of the sites are currently pending final approval for data sharing, and recently another 5 sites have been identified and have been invited to participate.

Following initial verbal agreements for collaboration, the GEMRIC was formally established at the first multi-site collaborative meeting in Bergen in June 2015. The GEMRIC was defined as a **G**lobal network for determining the mechanisms of action of **E**lectroconvulsive Therapy using **M**agnetic **R**esonance **I**maging through **C**ollaboration. During the first meeting, a data sharing agreement was developed that outlines the terms for contributing data to GEMRIC, policies for data storage/access and analysis. How to initiate new analysis of combined data was also established. A board was created consisting of lead researchers (e.g. Principle Investigators) from projects/studies participating in the collaboration. The GEMRIC board holds quarterly meetings to discuss projects and research in the network. The collaboration is coordinated from the University of Bergen, Norway, under the directorship of Dr. Leif Oltedal, where the Data Portal is located.

3.2. MRI data, clinical measures and common sample characteristics

A prerequisite for participating in the GEMRIC is that all contributing sites must have acquired and be willing to share longitudinal high-resolution MRI data in patients before and after receiving ECT. An overview of the current GEMRIC data set is given in Table 2. The combined number of patients is 345 with individual patient age ranging from 19 to 86 years (~60% female, ~85% unipolar depression). Nine of the sites also acquired control group(s). Six sites included three clinical and neuroimaging assessments (before, during, and immediately after the ECT series), and three sites included a fourth clinical and neuroimaging assessment up to six months post-ECT index. Eight sites obtained blood samples for analysis of genetic, genomic and other depression-related blood biomarkers during and after the ECT index. In addition, eight sites included longitudinal changes in cognition with neuropsychological assessments that included pre-morbid intelligence, cognitive screening, attention, language, memory, visuospatial, fluency, executive, and motor functions.

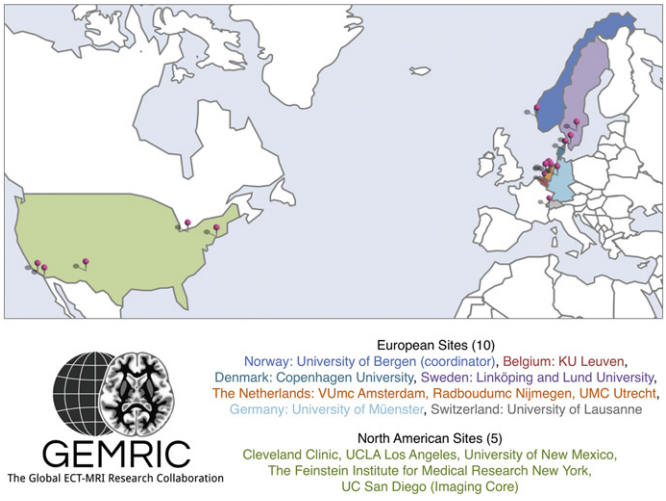

Fig. 1. Currently 15 sites are contributing to GEMRIC and more are expected to join, in line with growing interest in neuroimaging research in ECT. The UCSD site provides the Imaging Core and is responsible for tools for image processing at the common server located in Bergen.

Neuroimaging data was obtained at field strengths from 1.5 to 7 T using scanner hardware from three different vendors (GE, Philips, and Siemens). All sites included a volumetric T1-sequence in their protocol. Other imaging modalities included T2, fluid attenuated Inversion recovery (FLAIR), diffusion weighted imaging (DWI), resting state fMRI, task based fMRI, susceptibility weighted imaging (SWI) and magnetic resonance spectroscopy (MRS). In line with international guidelines, depressive symptoms were rated by the 17- or 24-item Hamilton Depression Rating Scale (HAM-D), or the Montgomery-Åsberg Depression Rating Scale (MADRS). For sites that used one depression rating scale, a validated equation converted HAM-D-17 to MADRS (Heo et al., 2007). Specific neurocognitive measures (semantic fluency, verbal list learning) may be compatible across sites for pilot data. Nine sites used mainly right unilateral stimulation (RUL), one site used bitemporal (BT) stimulation only, three sites used bilateral (BL) stimulation only, and one site used bifrontal (BF) stimulation only. The number of treatments per week was two or three for five and nine sites, respectively. Information on the mean number of treatments, pulse width, applied current, frequency and train duration is shown in Table 2.

3.3. Ethical, practical and technical challenges in forming the collaboration

Retrospective analysis of multi-site data poses several challenges. Local institutional review board (IRB) approvals may not have included data sharing and common analysis a priori, and equipment, scanners and software used for data acquisition, as well as patient inclusion and exclusion criteria, vary across participating sites.

3.3.1. Measures to ensure patient integrity

The fundamental first step for the GEMRIC collaboration is to ensure the relevant approvals from host institutions, institutional review boards, ethical committees or data protection authorities (collectively referred to as IRB). Details of rules and regulations differ between institutions and countries. While some sites had consent forms that included information about sharing of de-identified data and already had the necessary approvals, others needed to contact their local IRB. A standard, generic consent-form that may be used for sharing data to GEMRIC was developed. This form is used when local IRBs require new consent from each study participant. However, re-consent from patients is not always possible or necessary, and several other steps were suggested that could help fulfill local IRB requirements. Currently, for GEMRIC a) individual data is provided with new patient-IDs, b) each site retains the right to their own raw data, c) information about study site is hidden on the common server and in data analysis. In this large multi-site collection of subjects, the possibility of re-identifying individual study participants is thus very diminished. In such situations, data may for practical purposes be considered anonymous (Helsedirektoratet, 2013).

The Regional Ethic Committee South-East in Norway approved the inclusion of data from 500 individuals to the GEMRIC server located at the University of Bergen (2013/1032 ECT and neuroradiology, June 1st 2015). All data must be de-identified, and all collaborating sites must have a local IRB approval allowing them to share data with the server in Bergen. Although we regard more open data sharing as a future

Table 2
Characteristics of studies contributing to GEMRIC.
Overview of study specifics, patient characteristics, MRI protocol, ECT parameters, baseline and post-ECT measurements and blood biomarkers.

Center, key reference	Bergen, Norway (Oltedal et al., 2015a)	Amsterdam, the Netherlands (Dols et al., 2017)	Leuven, Belgium (Bouckaert et al., 2016a)	Copenhagen, Denmark (Jorgensen et al., 2016)	Lund, Sweden (Nordanskog et al., 2010)	Linköping, Sweden Nordanskog[b]	Albuquerque, NM USA (Abbott et al., 2014)	Nijmegen, the Netherlands (van Eijndhoven et al., 2016)	Los Angeles, CA, USA (Joshi et al., 2016)	Cleveland, OH, USA (Beall et al., 2012)	Utrecht, the Netherlands[b]	Lausanne, Switzerland Berlin, Germany (Dukart et al., 2014)	Glen Oaks, NY, USA (Argyelan et al., 2016)	Munster, Germany (Redlich et al., 2016)
Study specifics														
N	24[a]	34	34	19	12	11	41	23	43[a]	6	37[a]	10	23	28
MRI time points	4	3	3	3	4	3	2	2	4	2	2	3	3	2
Control group	+	+	−	−	−	−	+	+	+	−	+	+	+	+
Patient characteristics														
Mean age,	43.7 (14.6)	71.3 (9.8)	72.7 (7.6)	52.3 (11.3)	40.0 (16.0)	43 (14.7)	64.1 (9.1)	50.7 (8.5)	41.1 (14.2)	39.0 (5.4)	50.5 (13.9)	53.9 (10.7)	48.9 (13.8)	46.2 (10.2)
range	24–77	55–90	56–86	31–66	19–67	19–64	50–86	37–67	19–74	32–46	19–74	40–72	27–74	21–63
% female	67	59	65	68	83	55	63	65	61	33	68	62	35	61
% unipolar	75	100	100	68	50	100	100	100	86	100	86	50	87	100
MRI protocol														
Vendor	GE 3 T	GE 3 T	Philips 3 T	Siemens 3 T	Siemens 3 T	Philips 3 T	Siemens 3 T	Siemens 1.5 T	Siemens 3 T	Siemens 3 T	Philips 7 T	Siemens1.5 T	GE 3 T	Philips 3 T
Field strength														
sMRI, voxel (mm)	1.0 × 1.0 × 1.0	1.0 × 1.0 × 1.0	1.0 × 1.0 × 1.2	1.0 × 1.0 × 1.0	1.0 × 1.0 × 1.0	0.6 × 0.5 × 0.5	1.0 × 1.0 × 1.0	1.0 × 1.0 × 1.0	1.0 × 1.0 × 1.3	1.0 × 1.0 × 1.2	1.0 × 1.0 × 1.0	1.0 × 1.0 × 1.0	0.9 × 0.9 × 1.0	0.5 × 0.5 × 0.5
Multimodal	+	+	+	+	−	−	+	+	+	+	+	−	+	+
ECT parameters														
RUL, BL, BT, BF	RUL	32 RUL, 14 RUL–BL, 2 BL	34 RUL, 6 RUL-BL	BT	10 RUL, 2 RUL-BL	RUL	31 RUL, 10 RUL-BT	BL	37 RUL, 6 BL	BL	BL	RUL	BF	25 RUL, 3 RUL-BL
Sessions per week	3	2	2	3	3	3	3	2	3	3	2	2	3	3
# sessions in index	11 (3.6)	12.5 (7.8)	11.1 (3.1)	11.1 (3.2)	10.2 (2.9)	7.6 (2.7)	11.2 (3.2)	16.9 (6.2)	11 (3.8)	8.8 (3.9)	18.7 (9.9)	Until remission	6.3 (3.0)	14.1 (4.9)
Charge	Age and gender	Titration	Titration	Age and gender	Age and gender	Age and gender	Titration	Titration	Titration	Titration	Titration	Titration	1.5 seizure threshold	Age and gender
Pulse width	0.25–0.5	0.5–1.0	0.5–1.0	0.5–1.0	0.3–0.6	0.3–0.6	0.36–1.0	0.5–1.0	0.3–0.5	0.5	0.5	−	1.0	0.5

(ms)														
Current (mA)	900	−1000	−1000	900	800	800–900	900	-900	800–900	—	900	—	800	900
Frequency (Hz)	20–70	30–70	30–70	30–140	30–90	40–90	30–140	10–70	20–120	—	10–70	—	30–50	5–170
Stimulus duration (s)	6–8	2–10	2–10	2–8	6–8	6–8	2–8	2.8–8	1–8	—	6–8	—	0.5–2.3	2.8–8.0
Baseline measurements														
MADRS mean, range	32.6 (5.9) 18–44	33.9 (10.4) 14–50	35.2 (7.6) 22–50		37.8 (6.1) 29–50	35.5 (6.5) 26–49			38.1 (8.0) 22–54					30.68 (7.9) 17–52
HAM-D mean, range				27.6 (4.8)* 20–39			32.8 (7.8) 21–53	21.9 (5.3)* 12–32		25.2 (4.7)* 21–32	21.8 (7.2)* 10–37	21.8 (5.9) 10–29	28.7 (5.5) 21–45	21.7 (4.8) 13–35
Post index measurements														
MADRS mean, range	15.6 (8.7) 0–33	11.9 (9.6) 0–33	8.6 (10.1) 0–44		13.0 (10.5) 0–38	16.4 (11.0) 0–35			18.1 (11.4) 9–40					18.0 (10,7) 3–42
HAM-D mean, range				13.0 (6.5)* 0–25			8.8 (9.9) 0–35	12.6 (7.1)* 3–26		9.3 (3.7)* 5–14	14.9 (7.1)* 3–34	7.8 (7) 0–25	12.7 (8.9) 2–34	10.9 (6.6) 3–27
Blood draw time points	5	4	4	3	—	3	—	—	4	—	2	—	—	1

a)These sites are still including patients. b) Not published.
RUL: right unilateral, BL: bilateral, BT: bitemporal, BF: bifrontal, RUL-BL: changed from RUL to BL during treatment, MADRS: Montgomery Asberg Depressing Rating Scale, HAM-D: Hamilton Depression Scale using 24 items, * using 17 items. mm: millimeter, ms: milliseconds, mA: milliAmpere, Hz: Hertz, s: seconds.

goal, GEMRIC data is currently, due to IRB restrictions, only shared within the collaboration via the GEMRIC common analysis platform.

3.3.2. Common server and secure data storage

The GEMRIC dedicated server at the University of Bergen sits behind university firewall and requires two-factor authentication and VPN access for login. Data are analyzed on the server and displayed in a browser window through a Remote desktop connection. Raw data cannot be downloaded, but analysis and testing of hypotheses can be done online as the system has a powerful interface for statistical analysis with the R software package, version 3.3.1 (R Core Team, 2016). For details on the functionality of Data Portal see (Bartsch et al., 2014). The security level of our system, to our knowledge, exceeds that of similar systems, and the Data Portal software has been successfully used in other studies, e.g. the Pediatric Imaging, Neurocognition, and Genetics (PING) study (Jernigan et al., 2016).

3.3.3. Structural imaging preprocessing, FreeSurfer and Quarc analysis

In the pilot data described above used to test multi-site image preprocessing, the effect of distortion correction (Fig. 2A; single subject; scanner 1) was largest towards the apex of the skull where the manually measured dura-dura distance changed by ~8% ($p = 0.003$) and 2% ($p = 0.005$) for scanner 1 and 2, respectively (Fig. 2D). The calculated ECT-induced hippocampal volume change, based on automated FreeSurfer analysis, before and after correction was (μl, $n = 12$) 254 ± 304 ($p = 0.01$) and 339 ± 232 ($p = 0.0004$), representing a relative change of 3.4% and 4.7%, respectively. The reduced SD after corrections suggests reduced variance, which can also be appreciated in Fig. 2B. While ECT-induced hippocampal volume change was expected, the estimated

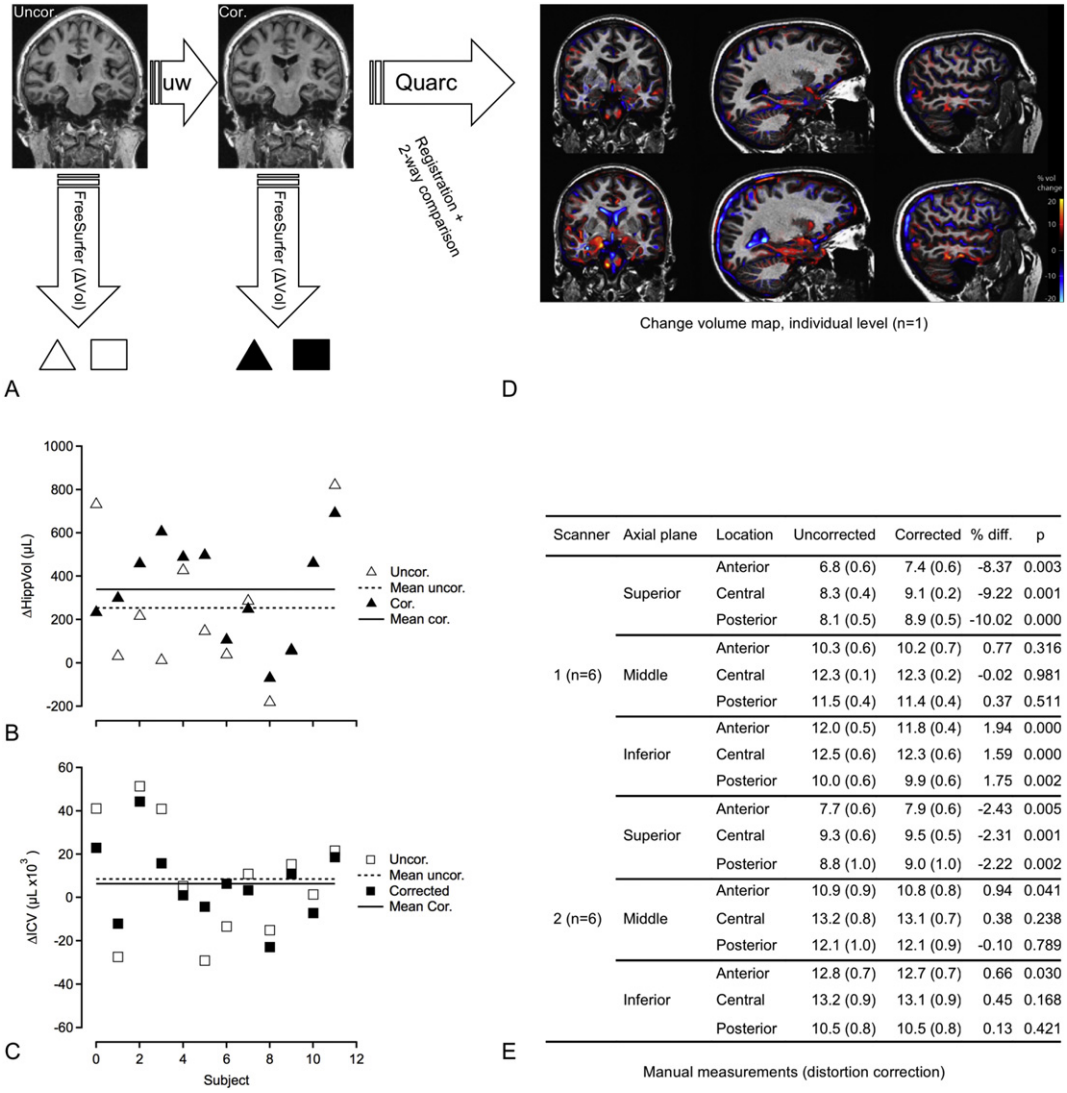

Scanner	Axial plane	Location	Uncorrected	Corrected	% diff.	p
1 (n=6)	Superior	Anterior	6.8 (0.6)	7.4 (0.6)	-8.37	0.003
		Central	8.3 (0.4)	9.1 (0.2)	-9.22	0.001
		Posterior	8.1 (0.5)	8.9 (0.5)	-10.02	0.000
	Middle	Anterior	10.3 (0.6)	10.2 (0.7)	0.77	0.316
		Central	12.3 (0.1)	12.3 (0.2)	-0.02	0.981
		Posterior	11.5 (0.4)	11.4 (0.4)	0.37	0.511
	Inferior	Anterior	12.0 (0.5)	11.8 (0.4)	1.94	0.000
		Central	12.5 (0.6)	12.3 (0.6)	1.59	0.000
		Posterior	10.0 (0.6)	9.9 (0.6)	1.75	0.002
2 (n=6)	Superior	Anterior	7.7 (0.6)	7.9 (0.6)	-2.43	0.005
		Central	9.3 (0.6)	9.5 (0.5)	-2.31	0.001
		Posterior	8.8 (1.0)	9.0 (1.0)	-2.22	0.002
	Middle	Anterior	10.9 (0.9)	10.8 (0.8)	0.94	0.041
		Central	13.2 (0.8)	13.1 (0.7)	0.38	0.238
		Posterior	12.1 (1.0)	12.1 (0.9)	-0.10	0.789
	Inferior	Anterior	12.8 (0.7)	12.7 (0.7)	0.66	0.030
		Central	13.2 (0.9)	13.1 (0.9)	0.45	0.168
		Posterior	10.5 (0.8)	10.5 (0.8)	0.13	0.421

E

Manual measurements (distortion correction)

Fig. 2. A) Coronal images before (uncorrected; left panel) and after (corrected; right panel) image processing with algorithm that corrects for gradient non-linearities (indicated by arrow "uw"), scanner 1. Change in FreeSurfer ROI (ΔVol) was calculated as the difference between ROI volume between the before- and after treatment scans for uncorrected (open symbols; △, □) and corrected data (filled symbols; ▲, ■). B) Change in hippocampal volume induced by ECT, estimated from data before- (Uncor.; △, ···) and after (Cor.; ▲,—) unwarping step. Notice increased mean effect size and reduced variance after distortion correction. C) Change in total intracranial volume from before to after treatment for data before- (Uncor.; □, ···) and after (Cor.; ■,—) unwarping step. There was no statistically significant change. Notice a tendency to reduced variance after corrections. D) Example of voxel based method (Quarc) showing areas of compression (blue) or expansion (red) between MRI time points. Upper panel; MRI ~2 h before and ~2 h after first ECT treatment (single session). Lower panel; MRI ~2 h before first ECT treatment and 7–14 days after ended treatment (multiple sessions). Notice larger changes after ended treatment (lower panel) with increased volume of the medial temporal lobe and reduced volume of the ventricles. E) Manual measurements done in Osirix MD from the axial plane at three different levels. The levels were: Inferior: The apex of pons. Middle: Ventral part of the genu corpus callosum. Superior: Halfway between the apex of the dura mater and the middle level. These levels were determined from the sagittal series. Then, the three levels were further divided by three lines which were used for the measurements. One halfway between the anterior and posterior boundaries of the dura mater. The two other lines halfway between the middle line and the anterior or posterior boundaries respectively. The lines were measured in cm. Significance (*P*-value) assessed by two-tailed *t*-test. [Fig. 2D is adapted from conference poster ISMRM 2015 abstract 705 (Oltedal et al., 2015b)].

intracranial volume was not changed after treatment. However, the variance seemed somewhat reduced after correction with an SD (in μl) of 26,921 and 17,838 before and after correction, respectively (Fig. 2C).

Regional anatomical change in longitudinal brain scan studies can be estimated using several available software packages. We have implemented Quarc which compares favorably with other methodologies for estimating structural change (Holland et al., 2012). An example is shown in Fig. 2D, illustrating regional change at the single subject level. This example corresponds with results found with FreeSurfer, and agrees well with visual inspection of accurately rigid-body co-registered slices from intra-individual T1 volumes before- and after ECT (not shown). Estimates of ECT induced volumetric change was further evaluated and compared to a group of healthy controls. The effect size (Cohen's *d*) of Quarc estimated regional cortical and subcortical change were typically in the range 0.5–2 (Fig. 3, Table 3). The pattern of change was broadly distributed, but the larger effect sizes were lateralized to the side of the ECT stimulus (all patients received right unilateral ECT); e.g. the volume change of the left and right temporal pole was 2.6% ($p < 0.05$) and 4.9% ($p < 0.001$), respectively ($n = 19$), compared to controls ($n = 9$). The mean standard deviation of change across ROIs for healthy controls (i.e. the "noise level"), scanned at time intervals similar to patients was ~0.8%. If scan corrections were not performed this value was ~0.9%; however, all controls were scanned on scanner 2, which has less geometric distortions than scanner 1, and this estimate will vary with scanner type. For the patient group both scanners were used, and we noticed that the effect of scan correction was larger for scanner 1 compared to scanner 2; the mean standard deviation across ROIs was 2.0 and 2.6% ($n = 6$) versus 1.8 and 1.9% ($n = 13$), for data with and without scan correction for scanner 1 versus scanner 2, respectively.

Based on the data from the Bergen sample (Fig. 3) we estimated sample sizes that will be needed to detect differences between groups for a few selected ROIs for effect sizes equal to Cohen's *d*, 25% of *d* and 10% of *d*. Estimates based on results from Quarc were compared with estimates based on corresponding results from the FreeSurfer longitudinal pipeline (Table 3).

3.3.4. GEMRIC projects

The common processing pipeline described above is used for initial harmonization and processing of GEMRIC imaging data. As specified in the GEMRIC data agreement, all board members can suggest projects of secondary data analysis by providing a one-page summary, including a timeframe. The suggestions are discussed by the board for consensus. By engaging the board, the proposal may get valuable feedback to improve impact. If future projects require other processing tools than the ones outlined here, this can be implemented on the server. The complete analysis pipeline, i.e. the computation, should then be packed in a Docker container (https://www.docker.com) which can be installed on the server.

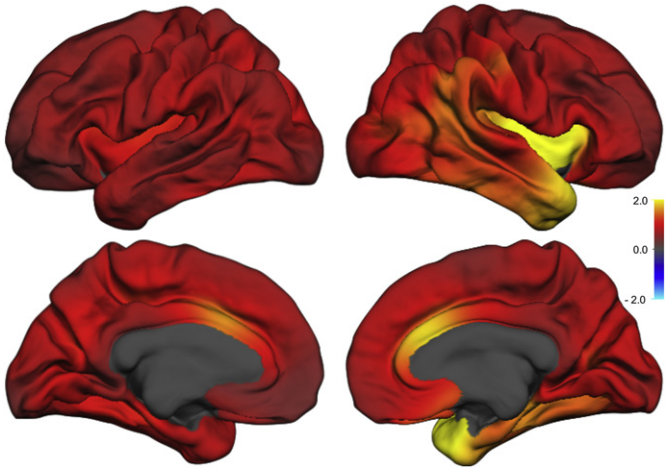

Fig. 3. Volumetric change map (Quarc; mean of $n = 19$) for lateral (upper row) and medial (lower row) aspect of left (left) and right (right) hemispheres. Scale bar represents Cohen's *d* effect size.

Table 3
Sample size estimates.
Sample size needed per study arm to detect differences in morphology between groups for selected ROIs. Cohen's *d* was calculated as mean change/SD. Power calculations were performed (G * Power version 3.1.9.2) for *t*-tests of difference between to independent means for groups with identical size. The error probability (α) was set to 0.01 and the power (1-β) was set to 0.8.

ROI, methodology	Mean Change			Sample size needed per arm		
	(%)	SD	Cohen's *d*	100% of *d*	25% of *d*	10% of *d*
Hippocampus, Quarc	2.43	1.77	1.37	15	204	1194
Hippocampus, FS long	1.63	1.42	1.15	20	280	1933
Caudal ant cingulate, Quarc	2.15	1.04	2.07	8	89	532
Caudal ant cingulate, FS long	1.94	1.77	1.10	22	323	1933
Sup temp gyrus, Quarc	1.99	1.68	1.18	19	280	1624
Sup temp gyrus, FS long	1.61	1.94	0.83	36	532	3652

4. Discussion

Though smaller hypothesis-driven studies are still considered useful to the field, several recently developed research initiatives (e.g., ENIGMA, the National Institute of Health Big Data to Knowledge (BD2K) initiative) emphasize the power of larger datasets to harvest diverse biomedical information for better understanding disease and treatment of disease. For example, by combining data from multiple origins one can account for site-specific effects and assess the relationship between individual factors and health outcomes while simultaneously offering greater generalization. Such datamining approaches, particularly those that combine different types of data (e.g., multimodal MRI measures, behavioral, clinical and demographic information as well as information of gene function), appear more likely to resolve the biological mechanisms accounting for successful antidepressant response and side effects. Likewise, sophisticated computational models applied to these datasets may identify biological markers extracted from imaging data that might predict future clinical response, risk of side effects or subsequent relapse to therapy, which would be of great translational value. Towards this end, the current paper describes the formation of GEMRIC and demonstrates the first common image processing pipeline. This international, multisite collaboration aims to leverage high-dimensional neuroimaging data combined with clinical and physiological data sources to determine the mechanisms and predictors of clinical response to ECT, mechanisms that are expected to overlap with other antidepressant treatments. Furthermore, in a large sample, patients who experience rare side effects may be captured – and such effects could possibly be related to imaging findings.

Several international collaborations that include neuroimaging data repositories have been formed recently (Eickhoff et al., 2016). These collaborations were used as a model to systematically establish the GEMRIC, the first international collaboration for longitudinal investigations of ECT that utilizes MRI. Our goal is to increase the knowledge about the mechanisms of action of ECT. To better understand the consequences and full width of structural brain changes with ECT, large sample sizes are needed. The current combined data pool is approximating a ten-fold increase relative to that of any single participating study, and more sites are expected to join in the near future. In our multi-site data set with individual-subject level data, we take advantage of standardized image processing and statistical tools to eliminate image analysis methods as a source of variance.

To reduce variance and scanner artefacts, the use of standardized processing streams is critical for pooled analysis of multi-centre data

(Cannon et al., 2014). One of the main causes of spatial distortions in MRI scans is non-linearity in the gradient fields that is used for spatial encoding. For longitudinal studies, correcting for gradient field distortions is important even for single-site studies, as the distortions depend on the position of the head within the main magnetic field. We have adapted automated correction procedures, developed at the Multi Modal Imaging Laboratory at UCSD, to correct for scanner specific effects (Jovicich et al., 2006) which may otherwise introduce bias and/or variance in the measures of anatomical change (Jernigan et al., 2016). Analysis of data from one site suggests that this processing step will reduce noise in measurements of longitudinal change. The method for estimating longitudinal change (Holland and Dale, 2011) calculates displacement maps bidirectional with respect to imaging time point, and avoids the inherent bias subject to some longitudinal change analysis methods (Fox et al., 2011; Holland et al., 2012; Thompson et al., 2011). By applying the pipeline to data from one site we show that large effect sizes of ECT-induced structural changes are achieved, with Cohen's *d* in the range 0.5–2. For comparison, the largest cross sectional meta-analysis of major depressive disorder to date found an effect size of −0.14 for patients' hippocampus volume relative to that of controls (Schmaal et al., 2016). In line with prior investigations (Holland and Dale, 2011; Holland et al., 2012), we use unbiased methods that maximizes the power for longitudinal anatomical change estimation. Using these methods, the current GEMRIC sample size should allow detection of differences in volume change that are at or above 25% of the effect sizes found in the Bergen sample (which is compared to healthy controls). Hence, we can take advantage of the heterogeneity of the sample (e.g. stimulus and treatment parameters, age, comorbidities, gender) to assess how site- or subject specific factors can modulate brain changes and health effects seen with ECT. We have presented our initial processing pipeline for structural data, but intend to include other modalities as well as alternative analysis approaches in the future.

Finally, the large combined sample size, with individual-subject data will be available to the collaboration and allow a rich set of hypothesis to be tested. Individual-subject data is a prerequisite for future investigations of ECT outcome prediction (Redlich et al., 2016), which may impact clinical patient care (Abbott et al., 2016), possibly enabling a more personalized approach to treatments.

Authors' contributions

LO drafted the manuscript and coordinated the work. UK and LO performed the systematic search. LErs, KJO, LO and CA contributed to the design. DH, HB and AMD developed the processing pipeline. OJE, HB, AMD and LO performed analysis. DH, AD, MLS, AMD, CA, LEm, PvE, IT, MA, PN, PH, MBJ, IES, SMH, BD, RR, UD, UK, HK, FB, PS, AA, RE, KN, KJO contributed data to Table 2 and/or in writing the manuscript, and all authors read an approved the final version.

Conflict of interest

Anders M. Dale is a Founder of and holds equity in CorTechs Labs, Inc., and serves on its Scientific Advisory Board. He is also a member of the Scientific Advisory Board of Human Longevity, Inc. (HLI), and receives funding through research agreements with General Electric Healthcare (GEHC) and Medtronic, Inc. The terms of these arrangements have been reviewed and approved by the University of California, San Diego in accordance with its conflict of interest policies. The other authors declare that they have no competing interests.

Indira Tendolkar has received speaker fees from Lundbeck.

Funding

This study is supported by Western Norway Regional Health Authority, Haukeland University Hospital and the University of Bergen, Norway. Additionally, individual sites acknowledge support from: The Lundbeck Foundation (MJB); the Münster Cohort was funded by the German Research Foundation (DFG, grant FOR2107, 1151/5-1 to UD) and Innovative Medizinische Forschung (IMF, RE111604 to RR); Centers of Biomedical Research Excellence (2P20GM103472-01 to CA); BD is supported by the Swiss National Science Foundation (NCCR Synapsy, project grant Nr 32003B_159780), Foundation Parkinson Switzerland and Foundation Synapsis. LREN is very grateful to the Roger de Spoelberch and Partridge Foundations for their generous financial support; for UCLA, funding was obtained through Award Numbers R01MH092301 and K24MH102743 from the National Institute of Mental Health.

Acknowledgements

We are thankful to the IT Department at the University of Bergen for providing the necessary IT infrastructure, and greatly appreciate the expert help and advice from Tore Linde and Anders Vaage in setting up the data sharing and distribution system and the Data Portal.

Appendix A. Supplementary information

Supplementary information to this article can be found online at http://dx.doi.org/10.1016/j.nicl.2017.02.009.

References

Abbott, C.C., Jones, T., Lemke, N.T., Gallegos, P., McClintock, S.M., Mayer, A.R., Bustillo, J., Calhoun, V.D., 2014. Hippocampal structural and functional changes associated with electroconvulsive therapy response. Transl. Psychiatry 4, e483.

Abbott, C.C., Loo, D., Sui, J., 2016. Determining electroconvulsive therapy response with machine learning. JAMA Psychiatry 73, 545–546.

Aoki, Y., Yamaguchi, S., Ando, S., Sasaki, N., Bernick, P.J., Akiyama, T., 2016. The experience of electroconvulsive therapy and its impact on associated stigma: a meta-analysis. Int. J. Soc. Psychiatry 62, 708–718.

APA, 2001. The practice of electroconvulsive therapy. Recommendations for Treatment, Training, and Privileging (A Task Force Report of the American Psychiatric Association), 2 ed. American Psychiatric Association, Washington, DC.

Argyelan, M., Lencz, T., Kaliora, S., Sarpal, D.K., Weissman, N., Kingsley, P.B., Malhotra, A.K., Petrides, G., 2016. Subgenual cingulate cortical activity predicts the efficacy of electroconvulsive therapy. Transl. Psychiatry 6, e789.

Arnone, D., Job, D., Selvaraj, S., Abe, O., Amico, F., Cheng, Y., Colloby, S.J., O'Brien, J.T., Frodl, T., Gotlib, I.H., Ham, B.J., Kim, M.J., Koolschijn, P.C., Perico, C.A., Salvadore, G., Thomas, A.J., Van Tol, M.J., van der Wee, N.J., Veltman, D.J., Wagner, G., McIntosh, A.M., 2016. Computational meta-analysis of statistical parametric maps in major depression. Hum Brain Mapp 37, 1393–1404.

Baker, M., 2016. 1,500 scientists lift the lid on reproducibility. Nature 533, 452–454.

Bartsch, H., Thompson, W.K., Jernigan, T.L., Dale, A.M., 2014. A web-portal for interactive data exploration, visualization, and hypothesis testing. Front. Neuroinform. 8, 25.

Beall, E.B., Malone, D.A., Dale, R.M., Muzina, D.J., Koenig, K.A., Bhattacharrya, P.K., Jones, S.E., Phillips, M.D., Lowe, M.J., 2012. Effects of electroconvulsive therapy on brain functional activation and connectivity in depression. J. ECT 28, 234–241.

Boccia, M., Acierno, M., Piccardi, L., 2015. Neuroanatomy of Alzheimer's Disease and Late-Life Depression: A Coordinate-Based Meta-Analysis of MRI Studies. J Alzheimers Dis 46, 963–970.

Bouckaert, F., De Winter, F.L., Emsell, L., Dols, A., Rhebergen, D., Wampers, M., Sunaert, S., Stek, M., Sienaert, P., Vandenbulcke, M., 2016a. Grey matter volume increase following electroconvulsive therapy in patients with late life depression: a longitudinal MRI study. J. Psychiatry Neurosci. 41, 105–114.

Bouckaert, F., Dols, A., Emsell, L., De Winter, F.L., Vansteelandt, K., Claes, L., Sunaert, S., Stek, M., Sienaert, P., Vandenbulcke, M., 2016b. Relationship between hippocampal volume, serum BDNF, and depression severity following electroconvulsive therapy in late-life depression. Neuropsychopharmacology 41, 2741–2748.

Bouckaert, F., Sienaert, P., Obbels, J., Dols, A., Vandenbulcke, M., Stek, M., Bolwig, T., 2014. ECT: its brain enabling effects: a review of electroconvulsive therapy-induced structural brain plasticity. J. ECT 30, 143–151.

Bora, E., Harrison, B.J., Davey, C.G., Yucel, M., Pantelis, C., 2012. Meta-analysis of volumetric abnormalities in cortico-striatal-pallidal-thalamic circuits in major depressive disorder. Psychological medicine 42, 671–681.

Cannon, T.D., Sun, F., McEwen, S.J., Papademetris, X., He, G., van Erp, T.G., Jacobson, A., Bearden, C.E., Walker, E., Hu, X., Zhou, L., Seidman, L.J., Thermenos, H.W., Cornblatt, B., Olvet, D.M., Perkins, D., Belger, A., Cadenhead, K., Tsuang, M., Mirzakhanian, H., Addington, J., Frayne, R., Woods, S.W., McGlashan, T.H., Constable, R.T., Qiu, M., Mathalon, D.H., Thompson, P., Toga, A.W., 2014. Reliability of neuroanatomical measurements in a multisite longitudinal study of youth at risk for psychosis. Hum. Brain Mapp. 35, 2424–2434.

Carney, S., Cowen, P., Dearness, K., Eastaugh, J., 2003. Efficacy and safety of electroconvulsive therapy in depressive disorders: a systematic review and meta-analysis. Lancet 361, 799–808.

Campbell, S., Marriott, M., Nahmias, C., MacQueen, G.M., 2004. Lower hippocampal volume in patients suffering from depression: a meta-analysis. Am. J. Psychiatry 161, 598–607.
Coffey, C.E., Figiel, G.S., Djang, W.T., Sullivan, D.C., Herfkens, R.J., Weiner, R.D., 1988. Effects of ECT on brain structure: a pilot prospective magnetic resonance imaging study. Am. J. Psychiatr. 145, 701–706.
Coffey, C.E., Weiner, R.D., Djang, W.T., Figiel, G.S., Soady, S.A., Patterson, L.J., Holt, P.D., Spritzer, C.E., Wilkinson, W.E., 1991. Brain anatomic effects of electroconvulsive therapy. A prospective magnetic resonance imaging study. Arch. Gen. Psychiatry 48, 1013–1021.
Cole, J., Costafreda, S.G., McGuffin, P., Fu, C.H., 2011. Hippocampal atrophy in first episode depression: a meta-analysis of magnetic resonance imaging studies. J. Affect. Disord. 134, 483–487.
Dale, A.M., Sereno, M.I., 1993. Improved localizadon of cortical activity by combining EEG and MEG with MRI cortical surface reconstruction: a linear approach. J. Cogn. Neurosci. 5, 162–176.
Desikan, R.S., Segonne, F., Fischl, B., Quinn, B.T., Dickerson, B.C., Blacker, D., Buckner, R.L., Dale, A.M., Maguire, R.P., Hyman, B.T., Albert, M.S., Killiany, R.J., 2006. An automated labeling system for subdividing the human cerebral cortex on MRI scans into gyral based regions of interest. NeuroImage 31, 968–980.
Diehl, D.J., Keshavan, M.S., Kanal, E., Nebes, R.D., Nichols, T.E., Gillen, J.S., 1994. Post-ECT increases in MRI regional T2 relaxation times and their relationship to cognitive side effects: a pilot study. Psychiatry Res. 54, 177–184.
Dols, A., Bouckaert, F., Sienaert, P., Rhebergen, D., Vansteelandt, K., Ten Kate, M., de Winter, F.L., Comijs, H.C., Emsell, L., Oudega, M.L., van Exel, E., Schouws, S., Obbels, J., Wattjes, M., Barkhof, F., Eikelenboom, P., Vandenbulcke, M., Stek, M.L., 2017. Early- and late-onset depression in late life: a prospective study on clinical and structural brain characteristics and response to electroconvulsive therapy. Am. J. Geriatr. Psychiatry 25, 178–189.
Du, M., Liu, J., Chen, Z., Huang, X., Li, J., Kuang, W., Yang, Y., Zhang, W., Zhou, D., Bi, F., Kendrick, K.M., Gong, Q., 2014. Brain grey matter volume alterations in late-life depression. J. Psychiatry Neurosci. 39, 397–406.
Dukart, J., Regen, F., Kherif, F., Colla, M., Bajbouj, M., Heuser, I., Frackowiak, R.S., Draganski, B., 2014. Electroconvulsive therapy-induced brain plasticity determines therapeutic outcome in mood disorders. Proc. Natl. Acad. Sci. U. S. A. 111, 1156–1161.
Eickhoff, S., Nichols, T.E., Van Horn, J.D., Turner, J.A., 2016. Sharing the wealth: neuroimaging data repositories. NeuroImage 124, 1065–1068.
Faul, F., Erdfelder, E., Lang, A.G., Buchner, A., 2007. G * Power 3: a flexible statistical power analysis program for the social, behavioral, and biomedical sciences. Behav. Res. Methods 39, 175–191.
Figiel, G.S., Coffey, C.E., Weiner, R.D., 1989. Brain magnetic resonance imaging in elderly depressed patients receiving electroconvulsive therapy. Convuls. Ther. 5, 26–34.
Fischl, B., Salat, D.H., Busa, E., Albert, M., Dieterich, M., Haselgrove, C., van der Kouwe, A., Killiany, R., Kennedy, D., Klaveness, S., Montillo, A., Makris, N., Rosen, B., Dale, A.M., 2002. Whole brain segmentation: automated labeling of neuroanatomical structures in the human brain. Neuron 33, 341–355.
Fischl, B., van der Kouwe, A., Destrieux, C., Halgren, E., Segonne, F., Salat, D.H., Busa, E., Seidman, L.J., Goldstein, J., Kennedy, D., Caviness, V., Makris, N., Rosen, B., Dale, A.M., 2004. Automatically parcellating the human cerebral cortex. Cereb. Cortex 14, 11–22.
Fox, N.C., Ridgway, G.R., Schott, J.M., 2011. Algorithms, atrophy and Alzheimer's disease: cautionary tales for clinical trials. NeuroImage 57, 15–18.
Girish, K., Jayakumar, P.N., Murali, N., Gangadhar, B.N., Janakiramaiah, N., Subbakrishna, D.K., 2001. Ect and t(2) relaxometry: a static walter proton magnetic resonance imaging study. Indian J. Psychiatry 43, 22–24.
Hamilton, J.P., Siemer, M., Gotlib, I.H., 2008. Amygdala volume in major depressive disorder: a meta-analysis of magnetic resonance imaging studies. Mol. Psychiatry 13, 993–1000.
Helsedirektoratet, 2013. Personvern og informasjonssikkerhet i forskningsprosjekter innenfor helse- og omsorgssektoren. Helsedirektoratet.
Heo, M., Murphy, C.F., Meyers, B.S., 2007. Relationship between the Hamilton Depression Rating Scale and the Montgomery-Asberg Depression Rating Scale in depressed elderly: a meta-analysis. Am. J. Geriatr. Psychiatry 15, 899–905.
Holland, D., Brewer, J.B., Hagler, D.J., Fennema-Notestine, C., Dale, A.M., Alzheimer's Disease Neuroimaging, I., 2009. Subregional neuroanatomical change as a biomarker for Alzheimer's disease. Proc. Natl. Acad. Sci. U. S. A. 106, 20954–20959.
Holland, D., Dale, A.M., 2011. Nonlinear registration of longitudinal images and measurement of change in regions of interest. Med. Image Anal. 15, 489–497.
Holland, D., McEvoy, L.K., Dale, A.M., Alzheimer's Disease Neuroimaging, I., 2012. Unbiased comparison of sample size estimates from longitudinal structural measures in ADNI. Hum. Brain Mapp. 33, 2586–2602.
Jack Jr., C.R., Bernstein, M.A., Fox, N.C., Thompson, P., Alexander, G., Harvey, D., Borowski, B., Britson, P.J., L.W., J., Ward, C., Dale, A.M., Felmlee, J.P., Gunter, J.L., Hill, D.L., Killiany, R., Schuff, N., Fox-Bosetti, S., Lin, C., Studholme, C., DeCarli, C.S., Krueger, G., Ward, H.A., Metzger, G.J., Scott, K.T., Mallozzi, R., Blezek, D., Levy, J., Debbins, J.P., Fleisher, A.S., Albert, M., Green, R., Bartzokis, G., Glover, G., Mugler, J., Weiner, M.W., 2008. The Alzheimer's disease neuroimaging initiative (ADNI): MRI methods. J. Magn. Reson. Imaging 27, 685–691.
Jernigan, T.L., Brown, T.T., Hagler Jr., D.J., Akshoomoff, N., Bartsch, H., Newman, E., Thompson, W.K., Bloss, C.S., Murray, S.S., Schork, N., Kennedy, D.N., Kuperman, J.M., McCabe, C., Chung, Y., Libiger, O., Maddox, M., Casey, B.J., Chang, L., Ernst, T.M., Frazier, J.A., Gruen, J.R., Sowell, E.R., Kenet, T., Kaufmann, W.E., Mostofsky, S., Amaral, D.G., Dale, A.M., Pediatric Imaging, N., Genetics, S., 2016. The pediatric imaging, neurocognition, and genetics (PING) data repository. NeuroImage 124, 1149–1154.
Jorgensen, A., Magnusson, P., Hanson, L.G., Kirkegaard, T., Benveniste, H., Lee, H., Svarer, C., Mikkelsen, J.D., Fink-Jensen, A., Knudsen, G.M., Paulson, O.B., Bolwig, T.G., Jorgensen, M.B., 2016. Regional brain volumes, diffusivity, and metabolite changes after electroconvulsive therapy for severe depression. Acta Psychiatr. Scand. 133, 154–164.
Joshi, S.H., Espinoza, R.T., Pirnia, T., Shi, J., Wang, Y., Ayers, B., Leaver, A., Woods, R.P., Narr, K.L., 2016. Structural plasticity of the hippocampus and amygdala induced by electroconvulsive therapy in major depression. Biol. Psychiatry 79, 282–292.
Jovicich, J., Czanner, S., Greve, D., Haley, E., van der Kouwe, A., Gollub, R., Kennedy, D., Schmitt, F., Brown, G., Macfall, J., Fischl, B., Dale, A., 2006. Reliability in multi-site structural MRI studies: effects of gradient non-linearity correction on phantom and human data. NeuroImage 30, 436–443.
Kempton, M.J., Salvador, Z., Munafo, M.R., Geddes, J.R., Simmons, A., Frangou, S., Williams, S.C., 2011. Structural neuroimaging studies in major depressive disorder. Meta-analysis and comparison with bipolar disorder. Arch. Gen. Psychiatry 68, 675–690.
Kennedy, S.H., Milev, R., Giacobbe, P., Ramasubbu, R., Lam, R.W., Parikh, S.V., Patten, S.B., Ravindran, A.V., Canadian Network for, M., Anxiety, T, 2009. Canadian network for mood and anxiety treatments (CANMAT) clinical guidelines for the management of major depressive disorder in adults. IV. Neurostimulation therapies. J. Affect. Disord. 117 (Suppl. 1), S44-53.
Koolschijn, P.C., van Haren, N.E., Lensvelt-Mulders, G.J., Hulshoff Pol, H.E., Kahn, R.S., 2009. Brain volume abnormalities in major depressive disorder: a meta-analysis of magnetic resonance imaging studies. Hum. Brain. Mapp. 30, 3719–3735.
Kunigiri, G., Jayakumar, P.N., Janakiramaiah, N., Gangadhar, B.N., 2007. MRI T(2) relaxometry of brain regions and cognitive dysfunction following electroconvulsive therapy. Indian J. Psychiatry 49, 195–199.
Mander, A.J., Whitfield, A., Kean, D.M., Smith, M.A., Douglas, R.H., Kendell, R.E., 1987. Cerebral and brain stem changes after ECT revealed by nuclear magnetic resonance imaging. Br. J. Psychiatry 151, 69–71.
McKinnon, M.C., Yucel, K., Nazarov, A., MacQueen, G.M., 2009. A meta-analysis examining clinical predictors of hippocampal volume in patients with major depressive disorder. J. Psychiatry Neurosci. 34, 41–54.
NICE, 2009. Depression: the treatment and management of depression in adults (update). NICE Clinical Guideline. vol. 90. National Institute for Health and Clinical Excellence, London.
Nickl-Jockschat, T., Palomero Gallagher, N., Kumar, V., Hoffstaedter, F., Brugmann, E., Habel, U., Eickhoff, S.B., Grozinger, M., 2016. Are morphological changes necessary to mediate the therapeutic effects of electroconvulsive therapy? Eur. Arch. Psychiatry Clin. Neurosci. 266, 261–267.
Nordanskog, P., Dahlstrand, U., Larsson, M.R., Larsson, E.M., Knutsson, L., Johanson, A., 2010. Increase in hippocampal volume after electroconvulsive therapy in patients with depression: a volumetric magnetic resonance imaging study. J. ECT 26, 62–67.
Oltedal, L., Kessler, U., Ersland, L., Gruner, R., Andreassen, O.A., Haavik, J., Hoff, P.I., Hammar, A., Dale, A.M., Hugdahl, K., Oedegaard, K.J., 2015a. Effects of ECT in treatment of depression: study protocol for a prospective neuroradiological study of acute and longitudinal effects on brain structure and function. BMC Psychiatry 15, 94.
Oltedal, L., Kessler, U., White, N.S., Bartsch, H., Hansen, B., Ersland, L., Grüner, R., Kuperman, J., Holland, D., Hugdahl, K., Oedegaard, K.J., Dale, A., 2015b. Abstract 705: ECT-induced structural changes in the human brain; a case series. ISMRM 2015 Annual Meeting, Toronto, Canada.
Ota, M., Noda, T., Sato, N., Okazaki, M., Ishikawa, M., Hattori, K., Hori, H., Sasayama, D., Teraishi, T., Sone, D., Kunugi, H., 2015. Effect of electroconvulsive therapy on gray matter volume in major depressive disorder. J. Affect. Disord. 186, 186–191.
Pande, A.C., Grunhaus, L.J., Aisen, A.M., Haskett, R.F., 1990. A preliminary magnetic resonance imaging study of ECT-treated depressed patients. Biol. Psychiatry 27, 102–104.
Peng, W., Chen, Z., Yin, L., Jia, Z., Gong, Q., 2016. Essential brain structural alterations in major depressive disorder: A voxel-wise meta-analysis on first episode, medication-naive patients. J. Affect. Disord. 199, 114–123.
Puri, B., Oatridge, A., Saeed, N., Ging, J., McKee, H., Lekh, S., Hajnal, J., 1998. Does electroconvulsive therapy lead to changes in cerebral structure? Br. J. Psychiatry 173, 267.
R Core Team, 2016. R: A language and environment for statistical computing. R Foundation for Statistical Computing, Vienna, Austria https://www.r-project.org/.
Redlich, R., Opel, N., Grotegerd, D., Dohm, K., Zaremba, D., Burger, C., Munker, S., Muhlmann, L., Wahl, P., Heindel, W., Arolt, V., Alferink, J., Zwanzger, P., Zavorotnyy, M., Kugel, H., Dannlowski, U., 2016. Prediction of individual response to electroconvulsive therapy via machine learning on structural magnetic resonance imaging data. JAMA Psychiatry 73, 557–564.
Rush, A.J., Trivedi, M.H., Wisniewski, S.R., Nierenberg, A.A., Stewart, J.W., Warden, D., Niederehe, G., Thase, M.E., Lavori, P.W., Lebowitz, B.D., McGrath, P.J., Rosenbaum, J.F., Sackeim, H.A., Kupfer, D.J., Luther, J., Fava, M., 2006. Acute and longer-term outcomes in depressed outpatients requiring one or several treatment steps: a STAR*D report. Am. J. Psychiatry 163, 1905–1917.
Sartorius, A., Demirakca, T., Bohringer, A., Clemm von Hohenberg, C., Aksay, S.S., Bumb, J.M., Kranaster, L., Ende, G., 2016. Electroconvulsive therapy increases temporal gray matter volume and cortical thickness. Eur. Neuropsychopharmacol. 26, 506–517.
Schmaal, L., Veltman, D.J., van Erp, T.G., Samann, P.G., Frodl, T., Jahanshad, N., Loehrer, E., Tiemeier, H., Hofman, A., Niessen, W.J., Vernooij, M.W., Ikram, M.A., Wittfeld, K., Grabe, H.J., Block, A., Hegenscheid, K., Volzke, H., Hoehn, D., Czisch, M., Lagopoulos, J., Hatton, S.N., Hickie, I.B., Goya-Maldonado, R., Kramer, B., Gruber, O., Couvy-Duchesne, B., Renteria, M.E., Strike, L.T., Mills, N.T., de Zubicaray, G.I., McMahon, K.L., Medland, S.E., Martin, N.G., Gillespie, N.A., Wright, M.J., Hall, G.B., MacQueen, G.M., Frey, E.M., Carballedo, A., van Velzen, L.S., van Tol, M.J., van der Wee, N.J., Veer, I.M., Walter, H., Schnell, K., Schramm, E., Normann, C., Schoepf, D., Konrad, C., Zurowski, B., Nickson, T., McIntosh, A.M., Papmeyer, M., Whalley, H.C., Sussmann, J.E., Godlewska, B.R., Cowen, P.J., Fischer, F.H., Rose, M., Penninx, B.W., Thompson, P.M., Hibar, D.P., 2016. Subcortical brain alterations in major depressive disorder: findings from the ENIGMA major depressive disorder working group. Mol. Psychiatry 21, 806–812.

Scott, A.I.F., Douglas, R.H.B., Whitfield, A., Kendell, R.E., 1990. Time course of cerebral magnetic resonance changes after electroconvulsive therapy. Br. J. Psychiatry 156, 551–553.
Segi-Nishida, E., 2011. Exploration of new molecular mechanisms for antidepressant actions of electroconvulsive seizure. Biol. Pharm. Bull. 34, 939–944.
Sexton, C.E., Mackay, C.E., Ebmeier, K.P., 2013. A systematic review and meta-analysis of magnetic resonance imaging studies in late-life depression. Am. J. Geriatr. Psychiatry 21, 184–195.
Steele, J.D., Currie, J., Lawrie, S.M., Reid, I., 2007. Prefrontal cortical functional abnormality in major depressive disorder: a stereotactic meta-analysis. J. Affect. Disord. 101, 1–11.
Tendolkar, I., van Beek, M., van Oostrom, I., Mulder, M., Janzing, J., Voshaar, R.O., van Eijndhoven, P., 2013. Electroconvulsive therapy increases hippocampal and amygdala volume in therapy refractory depression: a longitudinal pilot study. Psychiatry Res. 214, 197–203.
Thompson, W.K., Holland, D., Alzheimer's Disease Neuroimaging, I., 2011. Bias in tensor based morphometry Stat-ROI measures may result in unrealistic power estimates. NeuroImage 57, 1–4.
van Eijndhoven, P., Mulders, P., Kwekkeboom, L., van Oostrom, I., van Beek, M., Janzing, J., Schene, A., Tendolkar, I., 2016. Bilateral ECT induces bilateral increases in regional cortical thickness. Transl. Psychiatry 6, e874.
Videbech, P., Ravnkilde, B., 2004. Hippocampal volume and depression: a meta-analysis of MRI studies. Am. J. Psychiatry 161, 1957–1966.
Whiteford, H.A., Degenhardt, L., Rehm, J., Baxter, A.J., Ferrari, A.J., Erskine, H.E., Charlson, F.J., Norman, R.E., Flaxman, A.D., Johns, N., Burstein, R., Murray, C.J., Vos, T., 2013. Global burden of disease attributable to mental and substance use disorders: findings from the Global Burden of Disease Study 2010. Lancet 382, 1575–1586.
Zhao, Y.J., Du, M.Y., Huang, X.Q., Lui, S., Chen, Z.Q., Liu, J., Luo, Y., Wang, X.L., Kemp, G.J., Gong, Q.Y., 2014. Brain grey matter abnormalities in medication-free patients with major depressive disorder: a meta-analysis. Psychol. Med. 44, 2927–2937.